Direct Evidence of a Nonorthogonal Magnetization Configuration in Single Crystalline $Fe_{1-x}Co_x/Rh/Fe/Rh(001)$ System

F. Yildiz,[1] M. Przybylski,[1,2,*] and J. Kirschner[1]

[1]Max-Planck-Institut für Mikrostrukturphysik, Weinberg 2, 06120 Halle, Germany
[2]Faculty of Physics and Applied Computer Science, AGH University of Science and Technology, Mickiewicza 30, 30-059 Kraków, Poland

(Received 21 January 2009; published 1 October 2009)

Tetragonal distortion in $Fe_{1-x}Co_x$ alloy films grown epitaxially on Rh(001) substrates results in a strong perpendicular magnetic anisotropy. Since the perpendicular magnetic anisotropy varies with the $Fe_{1-x}Co_x$ film composition, one can grow multilayer structures with ferromagnetic films sequentially showing either an in-plane (e.g., Fe) or out-of-plane (e.g., $Fe_{0.5}Co_{0.5}$) easy-magnetization axis. The Rh spacers mediate an interlayer coupling which couples the magnetizations either ferromagnetically or antiferromagnetically, depending on the spacer thickness. When the anisotropy energy is compatible to the coupling, it produces nonorthogonal magnetization configurations which vary under a small change of the external magnetic field.

DOI: 10.1103/PhysRevLett.103.147203 PACS numbers: 75.30.Gw, 73.21.Ac, 75.50.Bb

A magnetic field that changes the magnetic configuration in ferromagnetic multilayers may be simply detected by measuring the change in the resistance of the multilayer. However, in order to detect weak fields, the energy difference between different magnetization directions should be small. This kind of behavior is of great interest for technological applications like magnetic field sensors (e.g., [1]). Such a change of the configuration with a small magnetic field requires a weak interaction between the ferromagnetic (FM) layers, which is usually achieved by increasing the thickness of the nonferromagnetic spacer or by precisely tuning the spacer thickness to a node in the oscillatory exchange coupling [2,3].

Another concept refers to the competition between magnetic anisotropy and indirect exchange coupling resulting in a nonorthogonal magnetization when one of the FM layers shows in-plane anisotropy whereas the second one prefers to be magnetized out of plane [4]. The concept was examined by photoemission electron microscopy experiment on the Co/Cu/Ni/Cu(001) system [5], with no clear evidence of the magnetization configuration from the hysteresis loops [6]. Some attempt was also made for FeAu $L1_0$ multilayers of alternate out-of-plane and in-plane anisotropy showing how the current changes with the thickness of the Au spacer [7]. Perpendicularly magnetized FM films in such systems are limited to Ni and to technologically complicated ordered $L1_0$ phases of Fe and Co with noble metals like FeAu and FePt [8].

In this Letter, we report on a fully epitaxial $(Rh/Fe_{1-x}Co_x)_2$ exchange-coupled system which is grown at room temperature (RT) and utilizes strong perpendicular magnetic anisotropy (PMA) of Fe-Co alloy films. The multilayer is distorted due to its pseudomorphic growth on the Rh(001) substrate. The $Fe_{1-x}Co_x$ layers are separated by Rh nonmagnetic spacers which support the distortion. The $(Rh/Fe_{1-x}Co_x)_2$ on Rh(001) system shows a distortion of $c/a = 1.24$, which is near to the value of 1.22 for which a maximum uniaxial magnetic anisotropy energy was theoretically predicted [9]. It has been shown experimentally that the PMA around the $x = 0.5$ composition is sufficiently strong to outbalance the shape anisotropy and result in the perpendicular easy-magnetization axis of $Fe_{1-x}Co_x/Rh(001)$ films [10]. Since the PMA originates from the tetragonal distortion, the easy-magnetization axis can be kept perpendicular unless the structure is relaxed, i.e., even up to 20 ML (where ML stands for monolayers) of $Fe_{0.5}Co_{0.5}$ [10]. Moreover, the magnetic moments around the $x = 0.5$ composition are of the order of $2.1\mu_B$, which results in a 50% larger saturation magnetization than that of the FePt and FeAu compounds used for perpendicular recording [11].

The magnetic anisotropy in $Fe_{1-x}Co_x$ layers can be continuously varied by changing the alloy composition, x, and thus one can grow $(Rh/Fe_{1-x}Co_x)_N$ multilayer structures of alternating in-plane and out-of-plane anisotropy. In case there is no interlayer exchange coupling, every other magnetic layer ($Fe_{1-x}Co_x$, $0.4 < x < 0.6$) can have an easy-magnetization axis perpendicular to the multilayer plane, and the intermediate Fe or Co (i.e., for $x = 0$ and $x = 1$, respectively) layers can be magnetized in plane [10]. The $Rh/Fe_{1-x}Co_x$ sequence, as well as the corresponding magnetic configuration, can be repeated many times. The Rh spacers are expected to mediate an exchange coupling, which can orient the magnetizations either parallel or antiparallel, depending on the spacer thickness [2,12]. A competition between the interlayer coupling (which can be tuned by the Rh-spacer thickness) with in-plane anisotropy in the first and out-of-plane anisotropy in the second of the coupled films (which can be tuned by the film composition) offers a unique possibility to result in a nonorthogonal magnetization configuration. Moreover, we will show that even a small change to the magnetic field

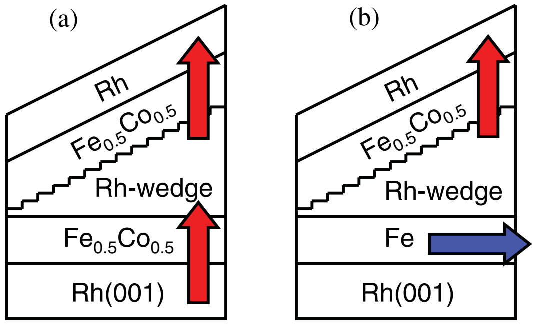

FIG. 1 (color). Schematic diagrams of the $Fe_{0.5}Co_{0.5}$/Rh-wedge(0–10 ML)/$Fe_{1-x}Co_x$/Rh(001) samples showing: (a) out-of-plane (for $x = 0.5$) and (b) alternating out-of-plane and in-plane (for $x = 0$) magnetic anisotropy.

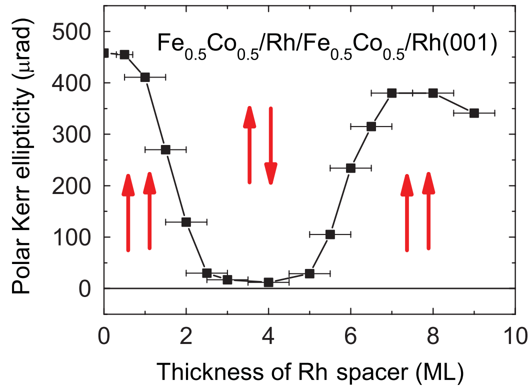

FIG. 2 (color). Polar Kerr ellipticity signal in remanence measured at RT for the $Fe_{0.5}Co_{0.5}$/Rh-wedge(0–10 ML)/$Fe_{0.5}Co_{0.5}$/Rh(001) sample with increasing Rh thickness. Since the thickness of both $Fe_{0.5}Co_{0.5}$ layers is almost the same, the signal from the AFM-coupled regions of the sample does not contribute to the measured Kerr signal.

can lead to a remarkable change of the magnetic configuration.

The $(Rh/Fe_{1-x}Co_x)_2$ multilayers were grown on Rh(001) at RT by molecular beam epitaxy in a multichamber ultrahigh vacuum system with less than 2×10^{-10} mbar during deposition. The $Fe_{0.5}Co_{0.5}$ films were grown using two effusion cells as described previously [13]. Magnetic properties were probed by utilizing the *in situ* magneto-optical Kerr effect (MOKE), for 1.85 eV photon energy of *s*-polarized light, both in polar and longitudinal geometry (incidence angle of 69° and 21° to the sample normal, respectively) at RT and the external magnetic field up to 0.7 T. A 0.5-mm-size laser beam allows us to follow the continuous changes in the magnetic properties along the Rh wedge.

In order to gain some insight into the coupling between two perpendicularly magnetized layers across a Rh spacer, we have grown a bilayer sample of $Fe_{0.5}Co_{0.5}$ films (each one 5 ML thick) separated with a Rh wedge [Fig. 1(a)]. The polar Kerr ellipticity loops were measured at RT by moving the sample towards the thicker Rh wedge. Within the available magnetic field, simple rectangular loops of small coercivity and a varying saturation signal or no loops were measured. Since the thickness of both $Fe_{0.5}Co_{0.5}$ layers is the same, their magnetizations are expected to be very similar. This is why no minor Kerr hysteresis loop from the AFM-coupled bilayer can be detected and why there is no contribution to the overall Kerr signal. Since the Kerr signal from the sample is integrated over the area of the laser beam size, both FM- and AFM-coupled regions of the sample are probed. The transition from the AFM- to the FM-coupled regions is not sharp and extends over a Rh thickness of 1–2 ML due to the roughness. The decreasing (or increasing) Kerr signal is a result of the decreasing (or increasing) contribution from the FM-coupled bilayer to the probed sample area. This is equivalent to the increasing (or decreasing) contribution from the AFM-coupled bilayer and finally must be interpreted as an oscillatory interlayer coupling (oscillating from AFM to FM coupling depending on the spacer thickness). As is seen from Fig. 2, a first maximum of the AFM coupling corresponds to the Rh thickness of about 4 ± 1 ML, whereas the Rh thickness of 7 ML relates to the FM coupling. The coupling changes within a distance of about 3 ML, which agrees with the distance of 2.7 ML observed for in-plane magnetized Co films separated by Rh [14].

In order to prove experimentally that nonorthogonal magnetization configurations can exist due to a competition between the anisotropy and the exchange coupling energies, a Rh/$Fe_{0.5}Co_{0.5}$/Rh-wedge/Fe/Rh(001) structure was grown [Fig. 1(b)]. The Fe layer is 8 ML thick and shows an in-plane easy-magnetization axis when grown as a single layer on Rh(001). This thickness of the Fe layer was chosen to be sure that the film is ferromagnetic with a well-defined magnetic anisotropy at RT [T_c of Fe films on Rh(001) decreases strongly with decreasing film thickness]. Growing the Fe film thicker could result in a structural relaxation and difficulties with growing the Rh layer epitaxially. The Fe layer was saturated in plane after growth and a single domain state has been achieved. The $Fe_{0.5}Co_{0.5}$ film is 6 ML thick and shows a perpendicular easy-magnetization axis when grown as a single layer on Rh(001). The Rh-spacer thickness varies from 0 to 10 ML within the distance of the sample width, i.e., 5 mm. This means that within the laser spot diameter (0.5 mm), the Rh-spacer thickness changes on average by 1 ML. The corresponding polar and longitudinal Kerr ellipticity loops are shown in Figs. 3–5. It can be immediately seen that the interlayer coupling plays an important role in determining the final magnetization configuration (which differs from the 90° configuration expected in the absence of interlayer coupling).

At the Rh thickness of 2–5 ML corresponding to AFM coupling.—The AFM interlayer coupling takes magnetizations from the easy-magnetization axes and tries to orient them antiparallel (keeping both the in-plane and perpendicular components of magnetization in antiparallel orientation). For strong AFM coupling at zero perpendicular

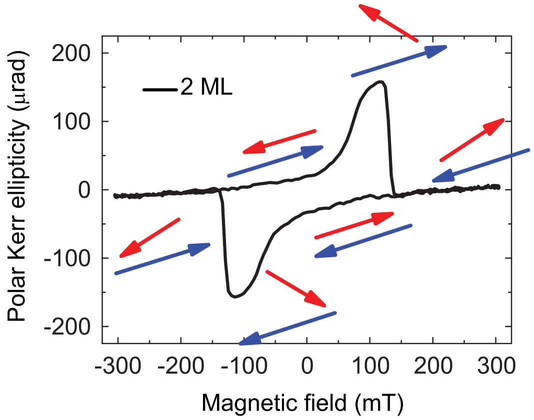

FIG. 3 (color). Polar minor Kerr ellipticity loop measured for $Rh/Fe_{0.5}Co_{0.5}/Rh/Fe/Rh(001)$ sample. The thickness of the Rh spacer is 2 ML and relates to the AFM coupling. The Fe layer is 8 ML thick, showing an in-plane easy-magnetization axis when grown on Rh(001) as a single film. The $Fe_{0.5}Co_{0.5}$ film is 6 ML thick, showing a perpendicular easy-magnetization axis when grown on Rh(001). The arrows indicate the magnetization of the $Fe_{0.5}Co_{0.5}$ layer (red) and of the Fe layer (blue), respectively.

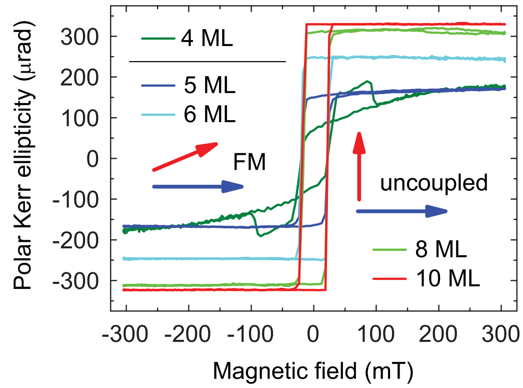

FIG. 4 (color). Polar Kerr ellipticity loops measured for the $Rh/Fe_{0.5}Co_{0.5}/Rh$-wedge/Fe/Rh(001) sample. The thickness of the Rh spacer increases up to 10 ML. The Fe layer is 8 ML thick, whereas the $Fe_{0.5}Co_{0.5}$ film is 6 ML thick. The loops evolve with increasing Rh thickness due to increasing contribution from the FM coupled bilayer and then from the uncoupled top $Fe_{0.5}Co_{0.5}$ layer to the total Kerr signal.

field, both Fe and $Fe_{0.5}Co_{0.5}$ film magnetizations are oriented antiparallel and thus only a small contribution to the polar Kerr signal in remanence exists (Fig. 3). With an increasing (positive) perpendicular field, the magnetization of the top $Fe_{0.5}Co_{0.5}$ layer rotates towards the film normal following the field direction and its easy-magnetization axis (Fig. 3). When the field approaches a certain value, the magnetization of the bottom Fe film switches to a more or less antiparallel orientation with the top $Fe_{0.5}Co_{0.5}$ layer in order to keep the AFM coupling, which is energetically more favorable. The polar field of this transition is of the order of 140 mT. Consequently, above this switching field, the polar component of the $Fe_{0.5}Co_{0.5}$ magnetization (positive) cancels the polar component of the Fe magnetization (negative), the net polar signal decreases to approximately zero, and a reversedlike loop is measured (Fig. 3). Such magnetization switching would not be observed, e.g., for a thicker Fe film, since the total magnetic energy balance could favor a different magnetization configuration in that case.

At the transition from AFM to FM coupling.—In polar geometry the loops show two components: reversed and "normal." This is because the loops (shown in Figs. 3 and 4) are integrated over the area probed by the laser beam. Within this area (the laser spot diameter is 0.5 mm) the thickness of the Rh spacer can vary, resulting in an interlayer coupling varying from AFM to FM (or to no coupling when tuned to the node in the oscillatory coupling). The reversed loop corresponds to the $Fe_{0.5}Co_{0.5}$ and Fe films being AFM coupled (as discussed above). The normal small coercivity loop corresponds to the FM or to no coupling between the $Fe_{0.5}Co_{0.5}$ and Fe films.

The loops experience significant changes when the interlayer coupling changes from AFM to FM, i.e., with increasing thickness of the Rh spacer (see Fig. 4). The reversedlike component to the overall polar Kerr signal disappears above a Rh-spacer thickness of 4 ML. The "normal" polar component at this Rh-spacer thickness is smaller than expected for the perpendicularly magnetized top $Fe_{0.5}Co_{0.5}$ layer. This shows explicitly that the magnetization of the top layer is not perpendicular but tilted to the sample plane due to the interlayer FM coupling (unfortunately, a quantitative analysis is difficult from the MOKE experiment). Since it is not possible to orient both magnetizations parallel, the FM coupling is recognized to be weaker than the AFM coupling at the thinner Rh-spacer layer. However, the coupling is sufficiently strong to keep the magnetic configuration almost unchanged in the polar magnetic field increasing up to 300 mT (Fig. 4).

At Rh thickness of 6–8 ML corresponding to FM coupling and above 9 ML at which there is no coupling.—Above an Rh thickness of 4–5 ML, the magnetization configuration is determined by the FM coupling. This leads to an increase of the polar signal. With a further increase of the Rh thickness (above 7 ML), the FM-coupling decreases, which again results in an increase of the polar signal (the corresponding polar Kerr ellipticity loops are shown in Fig. 4). At the Rh thickness of 9 ML, the polar signal reaches its maximum, which is equivalent to the signal from the $Fe_{0.5}Co_{0.5}$ film of exactly the same thickness when grown on Rh(001) as a single ferromagnetic layer. This corresponds to the case where the magnetizations of the Fe and $Fe_{0.5}Co_{0.5}$ films are not coupled and each of them is oriented along its own easy-magnetization axis.

In longitudinal geometry, the signal measured at low fields for a Rh-spacer thickness corresponding to FM coupling is large: the corresponding ellipticity is of the order of magnitude expected for the polar, but not for the longitudinal, Kerr effects (Fig. 5). This is because the switching of the Fe layer is associated with the switching of the tilted

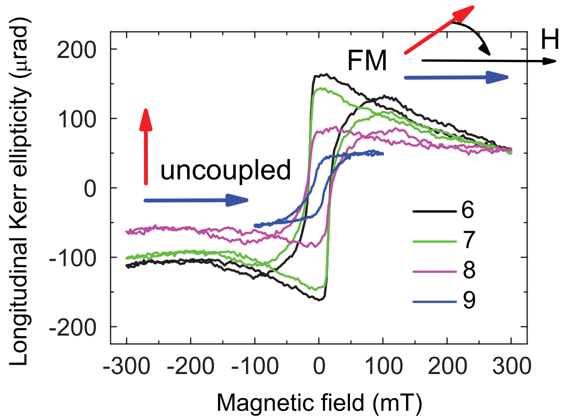

FIG. 5 (color). Longitudinal Kerr ellipticity loops measured for the $Rh/Fe_{0.5}Co_{0.5}$/Rh-wedge/Fe/Rh(001) sample. The thickness of the Rh spacer increases up to 10 ML. Switching the magnetization of the $Fe_{0.5}Co_{0.5}$/Rh/Fe bilayer in longitudinal geometry is associated with switching of the polar component, which contributes more and thus dominates the overall Kerr signal. For uncoupled $Fe_{0.5}Co_{0.5}$/Rh/Fe bilayer, the in-plane applied magnetic field does not switch the perpendicular magnetization of the top $Fe_{0.5}Co_{0.5}$ layer.

magnetization of the $Fe_{0.5}Co_{0.5}$ layer, i.e., also of its polar component. Actually, polar MOKE is detected here, which contributes strongly to the Kerr signal measured in longitudinal geometry. Another confirmation that the measured signal corresponds to the polar Kerr effect comes from the decreasing signal with increasing magnetic field. Since the field is applied in the sample plane, it forces the magnetization to follow the field direction. This reduces the polar component which in turn reduces the total signal detected in the longitudinal geometry.

The polar contribution to the MOKE signal measured in longitudinal geometry decreases when the thickness of the Rh spacer exceeds 7 ML. This is due to a smaller contribution from the FM-coupled part of the sample to the overall MOKE signal with the laser spot moving towards the thicker Rh-spacer layer, i.e., to the uncoupled part of the sample. When the Rh thickness corresponds to the uncoupled $Fe_{0.5}Co_{0.5}$/Rh/Fe bilayer, there is no reason to switch the perpendicular magnetization of the top $Fe_{0.5}Co_{0.5}$ layer by applying the in-plane magnetic field. When the magnetization of the $Fe_{0.5}Co_{0.5}$ film is finally oriented perpendicular to the film, only the longitudinal signal from the bottom Fe layer is measured (Fig. 5).

The interpretation remains in agreement with the interpretation of Fig. 2 which shows the polar Kerr ellipticity signal in remanence for the $Fe_{0.5}Co_{0.5}$/Rh-wedge(0–10 ML)/$Fe_{0.5}Co_{0.5}$/Rh(001) sample measured at RT. The only difference is that the magnetizations of both $Fe_{0.5}Co_{0.5}$ layers are always collinear and the signal from the AFM-coupled regions of the $Fe_{0.5}Co_{0.5}$/Rh-wedge(0–10 ML)/$Fe_{0.5}Co_{0.5}$/Rh(001) sample does not contribute to the measured Kerr signal.

In conclusion, since the anisotropy of $Fe_{1-x}Co_x$ alloy films of fixed composition depends only on distortion, it can remain when the in-plane lattice constant is kept constant. This is why the perpendicular easy-magnetization axis is easily achieved in $(Rh/Fe_{1-x}Co_x)_2$/Rh(001) multilayers. Moreover, since the anisotropy for fixed tetragonal distortion depends only on the film composition, a multilayer with alternating magnetization from in plane (e.g., for $x = 0$, i.e., Fe) to out of plane (e.g., for $x = 0.5$, i.e., for $Fe_{0.5}Co_{0.5}$) can be grown. However, the Rh-spacer layer introduces an interlayer coupling that is sufficiently strong to force magnetizations of the Fe and $Fe_{0.5}Co_{0.5}$ layers to be oriented parallel or antiparallel, depending on whether the coupling is FM or AFM, respectively. Combined with magnetic anisotropy, this competition results in a nonorthogonal magnetization configuration varying with the varying Rh-spacer thickness. The nonorthogonal configurations are clearly reflected in the shape of the hysteresis loops measured in both polar and longitudinal geometries. It is shown that even a tiny difference in system energy, caused, e.g., by a small magnetic field, results in a remarkable change of the magnetic configuration. A more detailed picture could result from a depth resolved experiment like coherent nuclear resonant scattering of synchrotron radiation which is currently under preparation.

Enlightening discussions with Professor W. Keune and technical support from G. Kroder are acknowledged.

*mprzybyl@mpi-halle.mpg.de

[1] S. M. Thompson, J. Phys. D **41**, 093001 (2008).
[2] P. Grünberg, R. Schreiber, Y. Pang, M. B. Brodsky, and H. Sowers, Phys. Rev. Lett. **57**, 2442 (1986).
[3] G. Binasch, P. Grünberg, F. Saurenbach, and W. Zinn, Phys. Rev. B **39**, 4828 (1989).
[4] A. Taga, L. Nordström, P. James, B. Johansson, and O. Eriksson, Nature (London) **406**, 280 (2000).
[5] W. Kuch, X.-Y. Gao, and J. Kirschner, Phys. Rev. B **65**, 064406 (2002).
[6] G. Lauhoff, A. Hirohita, J. A. C. Bland, J. Lee, S. Langridge, and J. Penfold, J. Phys. Condens. Matter **11**, 6707 (1999).
[7] D. Wilgocka-Slezak, T. Slezak, B. Croonenborghs, M. Rots, W. Karas, K. Krop, N. Spiridis, and J. Korecki, J. Magn. Magn. Mater. **240**, 536 (2002).
[8] J. S. Chen, B. C. Lim, and J. P. Wang, J. Appl. Phys. **93**, 1661 (2003).
[9] T. Burkert, L. Nordström, O. Eriksson, and O. Heinonen, Phys. Rev. Lett. **93**, 027203 (2004).
[10] F. Yildiz, F. Luo, C. Tieg, R. M. Abrudan, A. Winkelmann, M. Przybylski, and J. Kirschner, Phys. Rev. Lett. **100**, 037205 (2008).
[11] D. Weller, A. Moser, L. Folks, M. E. Best, W. Lee, M. Toney, M. Schwickert, J.-U. Thiele, and M. Doerner, IEEE Trans. Magn. **36**, 10 (2000).
[12] F. Yildiz, M. Przybylski, and J. Kirschner, J. Appl. Phys. **105**, 07C312 (2009).
[13] A. Winkelmann, M. Przybylski, F. Luo, Y. Shi, and J. Barthel, Phys. Rev. Lett. **96**, 257205 (2006).
[14] S. S. P. Parkin, Phys. Rev. Lett. **67**, 3598 (1991).